Available online at www.sciencedirect.com
SCIENCE DIRECT®
Journal of Molecular Graphics and Modelling 24 (2006) 362–372
Journal of Molecular Graphics and Modelling
www.elsevier.com/locate/JMGM

Unveiling hidden features of orphan nuclear receptors: The case of the small heterodimer partner (SHP)

Antonio Macchiarulo [a], Giovanni Rizzo [b], Gabriele Costantino [a], Stefano Fiorucci [b], Roberto Pellicciari [a,*]

[a] *Dipartimento di Chimica e Tecnologia del Farmaco, Università di Perugia, via del Liceo 1, 06127 Perugia, Italy*
[b] *Dipartimento di Medicina Clinica e Sperimentale, Clinica di Gastroenterologia ed Epatologia, Università degli Studi di Perugia, via E dal Pozzo, 06122 Perugia, Italy*

Received 26 January 2005; received in revised form 29 September 2005; accepted 29 September 2005
Available online 9 November 2005

Abstract

The small heterodimer partner (SHP) is an atypical nuclear receptor lacking the N-terminal ligand-independent activation domain and the DNA binding domain. SHP acts as transcriptional inhibitor of a large set of nuclear receptors, among which ER, AR, CAR, RXR, GR, LXR and ERRγ. The repression mechanism of SHP involves several actions including competition with coactivators binding on the AF-2 of nuclear receptors and recruitment of transcriptional inhibitors such as EID-1. The investigation of the structure and repression mechanism of SHP is a challenging task for a full understanding of nuclear receptor interaction pathways and functions. So far, mutational analyses in multiple populations identified loss of function mutants of SHP gene involved in mild obesity, increased birth weight and insulin levels. Furthermore, experimental mutagenesis has been exploited to characterize the interactions between SHP and the transcriptional inhibitor EID-1. With the aim of gaining insight into the structural basis of SHP repression mechanism, we modelled SHP and EID-1 structures. Docking experiments were carried out to identify the EID-1 binding surface on SHP structure. The results obtained in this study allow for the first time a unique interpretation of many experimental data available from the published literature. In addition, a fascinating hypothesis raises from the inspection of the proposed SHP structure: the presence of a potential unexpected ligand binding site, supported by recently available experimental data that may represent a breakthrough in the design and development of synthetic modulators of SHP functions.

Keywords: Orphan nuclear receptors; Small heterodimer partner; Structure prediction; Homology modelling; De novo modelling; Protein docking

1. Introduction

Nuclear receptor superfamily consist of 48 members including (i) the endocrine receptors whose endogenous ligands include thyroid and steroid hormones, derivatives and metabolites of Vitamins A and D; (ii) orphan nuclear receptors whose endogenous ligands are yet to be discovered [1].

In the last years, a number of orphan nuclear receptors have been *adopted* by the discovery of naturally occurring or synthetic ligands [2]. For these receptors, it has been possible to suggest a link to their physiological functions. In general terms, the physiological functions of nuclear receptors are dependent on the selective regulation of the expression of target genes that are involved in specific cellular processes such as cell growth, differentiation, development and homeostasis [3,4].

All the members of the superfamily of nuclear receptors share a modular structure [4–7]. In particular, they have a highly conserved central DNA-binding domain (DBD); a N-terminal domain which contains the ligand-independent transcriptional activation function-1 (AF-1); a C-terminal domain or ligand binding domain (LBD) endowed with the ligand-dependent transcriptional activation function-2 (AF-2). The DBD contains two cysteine coordinated zinc-fingers which are responsible for DNA binding and dimerization. In particular, DNA binding occurs in specific nucleotide sequences within the target gene promoters which are termed hormone response elements. The N-terminal domain varies in

* Corresponding author. Tel.: +39 075 585 5120; fax: +39 075 585 5124.
E-mail address: rp@unipg.it (R. Pellicciari).

1093-3263/$ – see front matter © 2005 Elsevier Inc. All rights reserved.
doi:10.1016/j.jmgm.2005.09.016

length and amino acid composition and it is responsible for the ligand-independent activation of receptor's transcription function through the interaction with other nuclear factors. The LBD contains the endogenous ligand binding site and it is involved in the homo/hetero-dimerization and in the recruitment of coregulators [8,9]. In particular, the latter occurs through conformational shifts of the AF-2 helix (H12) of LBD upon ligand binding [10,11].

The small heterodimer partner (SHP) is an atypical member of the above superfamily [12,13]. Indeed, it lacks the ligand-independent activation domain and the DBD. Furthermore, no ligands, endogenous nor exogenous, have so far been identified. The expression of SHP gene is regulated by a number of nuclear receptors including bile acid receptor (FXR), steroidogenic factor-1 (SF-1), hepatocyte nuclear factor-4α (HNF-4α), liver receptor homolog-1 (LRH-1), estrogen receptor-α (ERα) and estrogen related receptor-γ (ERRγ) [14–17].

In particular, the up-regulation of SHP gene by FXR plays a pivotal role in the control of bile acid metabolism and cholesterol homeostasis through the following SHP-dependent repression of cholesterol 7 alpha-hydroxylase gene (CYP7A1) [16,18,19]. Furthermore, the discovery of mutations of SHP gene that are associated with mild hyperinsulinemia and obesity, pinpoints a role of SHP in the control of glucose metabolism [20,21].

The physiological effects of SHP occur through a direct interaction with a number of nuclear receptors and the following repression of their transcriptional activity. Hence, the control on the cholesterol homeostasis is achieved by the interaction of SHP with LRH-1 that positively regulates the expression of CYP7A1 [22]. In a similar way, glucose metabolism is controlled by the interaction of SHP with HNF-4α, a positive regulator of the insulin biosynthesis [23]. Other interaction partners of SHP are estrogen receptor (ER), androgen receptor (AR), constitutive androstane receptor (CAR), retinoid X receptor (RXR), liver X receptor (LXR), ERRγ, glucocorticoid receptor (GR), peroxisome proliferator-activated receptor-γ (PPARγ) [15,24–27]. Although SHP usually represses the transactivation of its interaction partners, it has been reported that SHP augments PPARγ transactivation [28]. Interestingly, the SHP mediated enhancement of the activity of PPARγ is linked to a direct interaction of SHP with the DBD of PPARγ. The repression mechanism of SHP involves at least two actions including: (i) competition with coactivators binding on the AF-2 of nuclear receptors and (ii) recruitment of unknown corepressors through its transrepression domain [23,29,30].

In particular, competition with coactivators binding on the AF-2 surface of interaction partners constitutes the molecular basis of the interaction between SHP and nuclear receptors. Briefly, the binding competition occurs through the interaction of three LxxLL-like motifs of SHP, also termed nuclear receptor (NR) boxes. Noteworthy, SHP was found to interact with ER through both NR boxes 1 and 2. [29] Conversely, the interaction of SHP with AR and GR is only mediated by NR box 2 [25,26]. These results suggest that the redundancy of NR boxes of SHP is an essential feature for a selective interaction with diverse nuclear receptors.

The second action of SHP involves the recruitment of corepressors leading to the formation of a hetero-trimer complex with nuclear receptors. Båvner et al. reported that the E1A-like inhibitor of differentiation-1(EID-1) is recruited by SHP as corepressor [30]. EID-1 is a nuclear protein which blocks p300 coactivation function and it is involved in the inhibition of muscle differentiation [31,32]. Interestingly, EID-1 does not interact directly with classical nuclear receptors, supporting the hypothesis of a hetero-trimer complex formation in which SHP acts as bridge between EID-1 and nuclear receptors.

According to Båvner and coworkers, the region encompassing residues 54–120 of EID-1 constitutes the SHP interaction domain and its relative binding surface is located on helices 3 and 12 of SHP. In addition, a recent report pinpointed that the loop region between helices 6 and 7 (residues 128–139) of SHP is also involved in defining the binding surface of the full length of EID-1 surface [32].

In the present study, we exploited homology modelling techniques to construct a 3D model of SHP. Furthermore, a protein fold was assigned to the SHP binding domain of EID-1 (residues 54–120) using ab initio structure prediction methods. The obtained structures were used to gain insight into the mechanism of SHP transcriptional repression. In particular, the recruitment of EID1 by SHP was studied in silico by mean of molecular docking experiments. The obtained results are discussed in the light of available experimental data. Being aware of the current limitations of the computational methods herein used, we thought that the investigation of such a model would help to clarify the repression mechanism of SHP and aid the design of potential modulators of SHP's functions.

2. Methodology

The alignment of the human small heterodimer partner (SHP, Entrez code: NP_068804) and Ultrasipracle (USP; pdb code 1g2n) sequences was performed using the Align123 module of Insight II [33]. The Blosum matrix was used with a gap penalty of 11 and a gap extension penalty of 1. Secondary structures were assigned according to PHD prediction server and the crystal structure, respectively [34]. The alignment was carefully checked to avoid gap insertion where conserved secondary structure motifs were present (Fig. 1a).

The 'Modeler' module of Insight II was used with the default setting to build 3D models of the LBD of SHP [35]. The large loop insertion (residues 110–138) was modelled using ab initio prediction methods (Robetta server) [36]. In details, a larger region encompassing residue 107–141 was submitted to fold recognition. The resulting 10 fold solutions were manually docked by fitting the alpha carbons of residues 107–109 and 139–141 onto the corresponding alpha carbons of SHP structure. The number of steric clashes between SHP and the overlaid residues 110–138 was calculated and used as energy score. After the above docking procedures, the optimal fold of region 110–138 was chosen among the Robetta solutions as the one presenting the best fit into the gap window of SHP and the best energy score. In particular, fold 1 presented a root mean

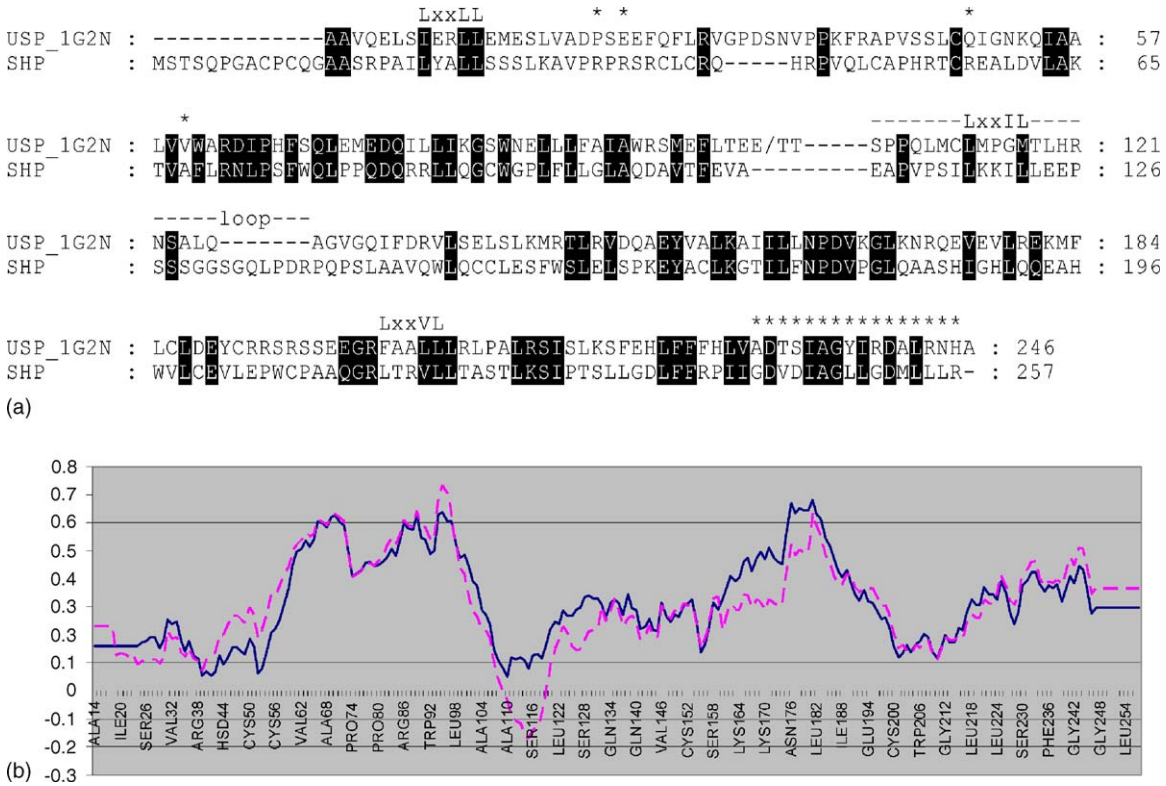

Fig. 1. (a) Alignment of USP (1g2n) and SHP sequences. Identities and strong similarities are black shaded. Nuclear receptor motifs (NR boxes) are highlighted. Residues experimentally involved in SHP repression mechanism are marked with star sign. The large region (residues 110–138) modelled using ab initio folding prediction methods is marked with dash sign. (b) Verify3D plot of final SHP structure (continuous line). Average score of alignments explored for region 110–138 (dash line).

square deviation (RMSD) of 2.90 and no steric clashes. Thus, a cut and paste procedure was applied to fold 1, deleting residues 107–109 and 139–141 and merging the remaining ones onto the SHP model following the docked pose of fold 1. The final homology model was submitted to minimization protocols using Charmm22 force–field. In particular, the G-Born approximation was considered to mimic the solvation effect [37]. The energy minimization was performed using a cycle of 500 steps of Steepest Descendent algorithm followed by several cycles of Conjugate Gradient algorithm until reaching a gradient of 0.01 Kcal/mol. A geometric validation of the 3D model was carried out using Procheck and Verify3D servers [38,39]. If present, bad geometries were manually corrected and the structure minimized again with the above protocol. The fold of the SHP binding domain of EID-1 (residues 54–120) was predicted using Robetta server [36]. Docking experiments were carried out using 3D-DOCK [40]. All the resulting docked solutions were scored using a residue pair potential score based on an empirical matrix generated from 103 non-homologous interfaces retrieved from protein databank (pdb). The electrostatic potential of SHP and EID-1 was calculated using the Finite Difference Poisson–Boltzmann method as implemented in Delphi module of Insight II software package [41].

Docking experiments of phospholipids into the putative binding pocket of SHP were performed using Autodock v3.0 [42]. The phosphatidylethanolamine was extracted from the pdb file of USP and refined with the target protein using the Autodocktools package. Briefly, 100 runs were carried out using the genetic algorithm with a population size of 50 individuals and 2,500,000 energy evaluations. If no specified, other parameters were left to their respective default values. The search was conducted in a grid of 60 points per dimension and a step size of 0.375. The grid was centred on the centre of mass of the residues defining the putative binding site (residues 48–49, 52, 55–56, 59, 92, 96–97, 100, 135–136, 138–141, 144–145, 230–231, 234–235, 238, 240). Results were clustered and ranked in terms of binding energy.

The top scoring solution yielded a binding energy of −18.66 kcal/mol and the lowest root mean square deviation from the bioactive conformation of phosphatidylethanolamine in USP (RMSD = 2.83). The corresponding docking pose is shown in Fig. 7b.

All computations were carried out on a SGI O2 R12000 workstation and AMD Athlon 1800+ MP based machine running Linux Slackware 9.0 operating system.

3. Results

3.1. Homology modelling of SHP

The sequence of human SHP (257 residues, Fig. 1a) was submitted to a BLAST [43] search versus the RCSB protein database using the WU-BLAST server [44]. The best hit

resulted in the ligand binding domain (LBD) of Ultraspiracle protein (USP; pdb code 1g2n; score = 167).

The same homologous protein was found among the best hits with an expectance value (*e*-value) below 1e−10 (at first iteration) and 1e−70 (at second iteration) using PSI-BLAST [45] runs.

Ultraspiracle protein (USP) is the ortholog of the vertebrate retinoid X receptor (RXR) in insects and mediates the heterodimerization of several nuclear receptors like RXR does in vertebrates [46].

In contrast to all known LBD of nuclear receptors, USP presents a unique feature: the loop connecting helix H1 to helix H3 (L1-3) folds around helices H3, H11 and H12 [47]. This particular fold locks the H12 in a resting state and prevents any of its conformational movements (Fig. 2).

Recently, Przibilla and coworkers reported that this antagonistic conformation of H12 is indispensable for the interaction between USP and the DNA [48].

Although a SHP model has been recently proposed by using the LBDs of HNF-4α and ERRγ as templates [49], we thought that USP could be a more suitable template to construct a 3D model of SHP given the following considerations. The sequences of the LBD of USP and SHP share 22% of identity and 38% of similarity (Fig. 1a). The C-terminus region of SHP is required for its transcriptional repression function [23]. This function occurs through the recruitment of transcriptional inhibitors by helix H12 [30]. In nuclear receptors, the recruitment of corepressors, such as NCoR, occurs through the stabilization of an antagonistic conformation of H12. Although SHP does not recruit NcoR [50], we thought that a similar mechanism may occur in SHP as well. In particular, helix H12 of SHP, which contains the AF-2 in nuclear receptors, would be locked in a resting conformation mimicking the antagonistic conformation of H12 found in the crystal structure of USP. This would explain why SHP behaves like a transcriptional repressor. Moreover, it should be reminded that the transcriptional enhancement of PPARγ by SHP has different molecular basis, by involving a direct interaction of SHP with the DBD of the nuclear receptor [28].

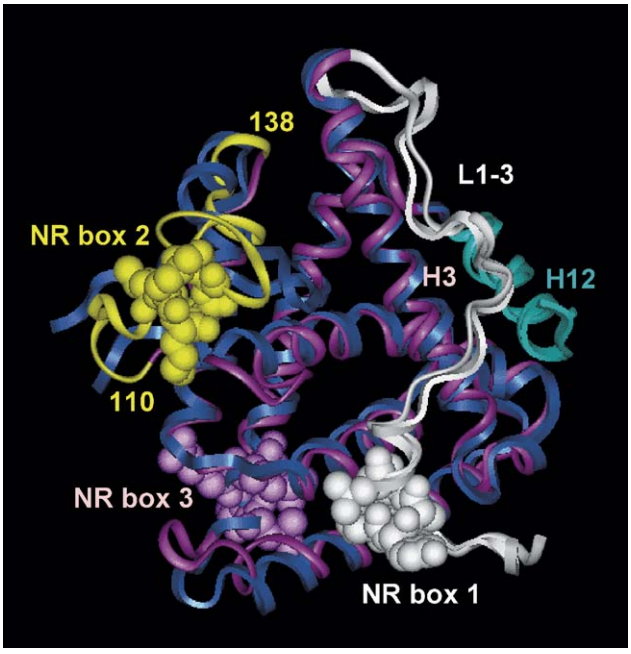

Fig. 2. Superposition of USP (blue) and SHP (magenta) structures. The N-terminal loop L1-3 folding around helices H3 and H12 (cyan) is colored in white. The region (110–138) modelled using ab initio folding prediction methods is colored in yellow. Residues belonging to NR boxes are shown in CPK.

Several alignments were explored to build the region encompassing residues 110–138. This region contains the NR box 2 (residues 118–122) and an insertion loop (residues 128–139) which was demonstrated to be involved in transcriptional inhibitor recruitment by SHP [49].

All the investigated alignments of this region failed in assigning a fold endowed with a positive score in the Verify3D fold validation test (Fig. 1b). Hence, the large non-conserved region (residues 110–138) containing the NR box 2 (residues 118–122) was modelled using ab initio folding prediction methods (Robetta server, see below) [36]. The resulting 10 fold solutions were manually docked onto SHP structure and the fold exhibiting the best fit into the gap window and the best energy score was assigned to the sequence of the above region (see Section 2 for details). Interestingly, the ab initio folding prediction method assigned an alpha helix conformation to residues 115–122 comprising the NR box 2. Evidences pinpoint that this is the correct fold for the NR boxes. In particular, NR boxes compete with coactivator binding on the AF-2 surface of nuclear receptors. Crystal structures of nuclear receptors in complex with coactivators (examples: 1gwq, 1gwr, 1mvc) reveal an alpha helix conformation assumed by coactivator peptide. Since the alpha helix conformation is the bioactive conformation assumed by coactivators to interact with nuclear receptors, it is conceivable that NR boxes would assume a similar bioactive conformation to compete with their binding on the AF-2 surface. Very recently, a crystal structure of NR box 1 of SHP in complex with liver receptor homolog-1 (LRH-1) has been solved [51]. The crystal structure confirms the above assumption revealing that the NR box 1 occupies the coactivator binding site of LRH-1 and adopts an alpha helix conformation.

NR boxes 1 (residues 21–25) and 3 (residues 202–206) were also set to alpha helix conformations according to the relative secondary structure elements of aligned residues in USP.

The resulting 3D model of SHP was geometrically validated and its folding was checked using the Verify3D server (Fig. 1b).

3.2. Fold assignment of the SHP binding domain of EID-1

The sequence of the SHP binding domain of EID-1 (residues 54–120) was submitted to sequence similarity searches using WU-BLAST [43] and PSI-BLAST [45] versus the RCSB protein database. No sequence homologs were found with good confidence values (*e*-values > 1). Then, we submitted the domain of EID-1 to fold recognition (threading) servers (3D-PSSM [52], FFAS03 [53], FUGUE2 [54], INUB [55], mGenTHREADER [56], SUPERFAMILY [57], 3D-JURY

and MetaBasic [58]) to identify structural homologs. Again, all runs did not yield any result with a good prediction confidence.

Hence, the sequence of the SHP binding domain of EID-1 (residues 54–120) was submitted to Robetta server for ab initio prediction of its tertiary structure [36]. Briefly, the above server uses the Rosetta algorithm to perform de novo modelling of protein's domains when no structural homolog is known. It is based on fragment insertion along the full length of the primary sequence to explore the conformational space of a given domain. This operation ends up with the production of a large ensemble of decoy from which the final models are selected. Robetta server was satisfactorily tested in blind predictions of target proteins at CASP5 and CAFASP3 experiments [59]. In our study, a total of 10 possible folds were assigned to the SHP binding domain of EID-1 (Fig. 3). Models 1–9 represent the centre of the most populated clusters of sequence's folding space. Model 10 is the lowest energy decoy that did not belong to the previously represented clusters. Table 1 shows some structural descriptors relative to each model.

Table 1
Structural descriptors calculated for the 10 models of EID-1 fold

Fold	RMSD (Cα–Cα)[a]	Radius of gyration[b]	ASA (Å^2)[c]	Residue[d] (%)
Model 1	0.0	11.97	4877	92.3–6.2
Model 2	5.4	11.25	4762	93.8–6.2
Model 3	6.0	11.79	4952	93.8–6.2
Model 4	5.0	11.00	4546	93.8–3.1
Model 5	6.4	11.55	4734	96.9–3.1
Model 6	9.1	11.27	4768	95.4–4.6
Model 7	9.3	10.78	4322	96.9–3.1
Model 8	4.8	11.22	4825	96.9–3.1
Model 9	6.3	11.84	5120	96.9–3.1
Model 10	11.0	10.88	4672	96.9–3.1

[a] Root mean square deviation (RMSD) of alpha carbons using model 1 as target structure.
[b] The radius of gyration is defined as the mass weighted root mean square distance of a collection of atoms from their common centre of mass.
[c] Solvent accessibile surface area.
[d] Number of residues in favoured–allowed regions of Ramachandran plot.

3.3. In silico recruitment of EID1 by SHP

The 10 folds assigned to the SHP binding domain of EID-1 were docked onto the LBD structure of SHP. The results obtained from the resulting 10 docking experiments were ranked using the residue pair potential score. The top 50 solutions for each docking experiment were retrieved. The spatial distribution of the resulting 500 complexes around the structure of SHP was studied in order to identify the putative binding surface of EID-1 on SHP. In all of the 500 complexes, EID-1 is clustered mainly around the helix H12 of SHP (Fig. 4).

To gain insights into the molecular basis of these interactions, we selected the best ranked solution for each model of EID-1. We thought that the model presenting the highest score of interaction with SHP would resemble the most likely fold of EID-1 (Table 2). In particular, complexes of SHP

(a)
1 MAEMAELCELYEESNELQMDVLPGEGYMEVGRGARWPAPEEGPMEEEAGPAAARAQRGLF
61 PEAGA**D**L**E**G**DE**F**DD**W**EDD**Y**E**FP**EEE**RWSGAMHRVSAALEEANKVFLRTARAGDALDGGFQ
121 ARCEKSPFDQLAFIEELFSLMVVNRLTEELGCDEIIDRELMLTREEETT

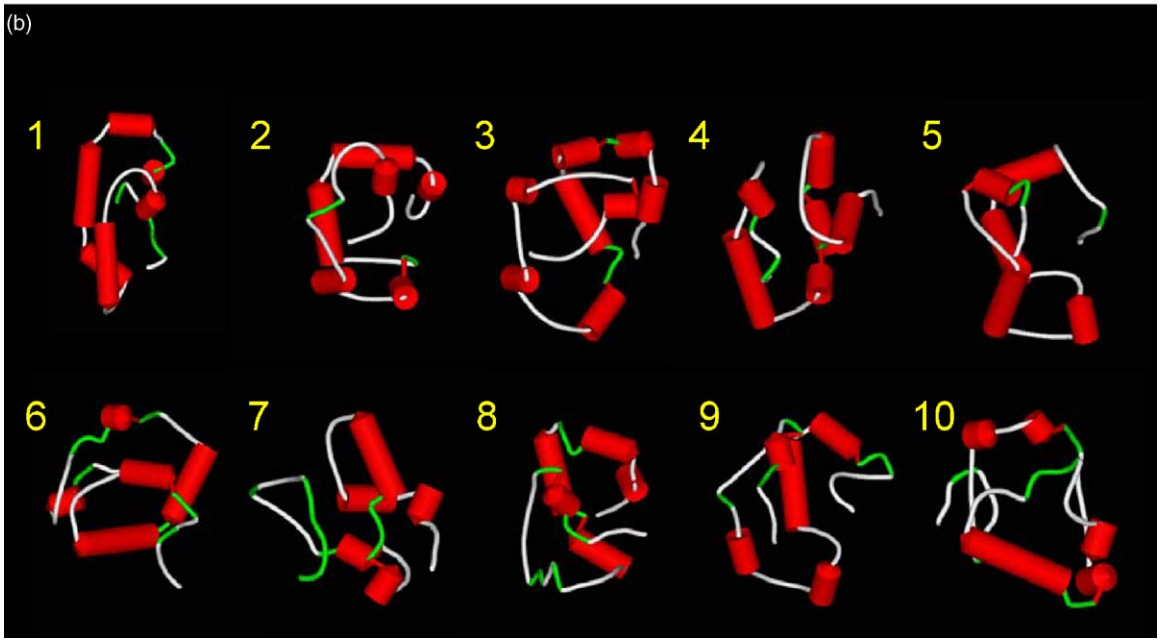

Fig. 3. (a) Sequence of EID-1 (mus musculus). Residues belonging to SHP binding domain are underlined. An acidic stretch of glutamic and aspartic residues is bold typed. (b) Models of EID-1 fold resulting from Robetta server.

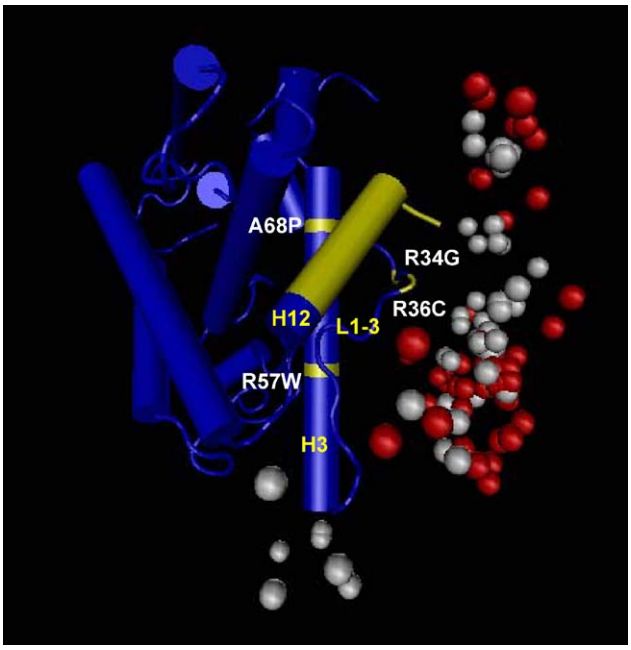

Fig. 4. Docking solutions of EID-1 and SHP. Each ball represents the centre of mass of one docked solution. For clarity, only the top 50 solutions of model 8 (red) and model 10 (white) are shown.

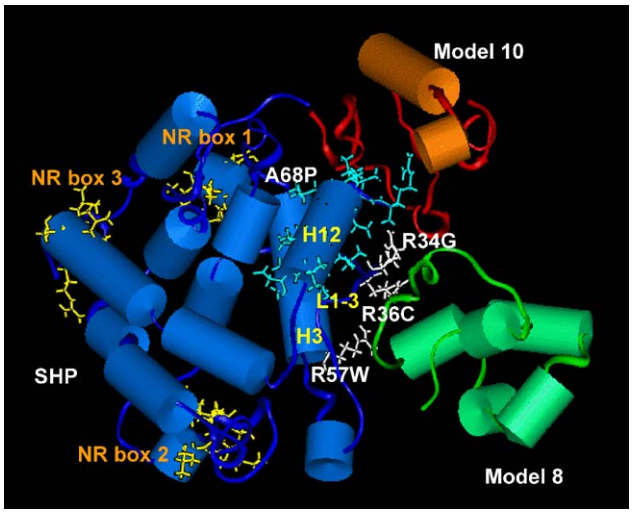

Fig. 5. Docking solutions of model 8 (green) and 10 (orange) of EID-1 onto the binding surface of SHP. Secondary structural motifs and residues of SHP defining the binding surface are highlighted. The regions where the interaction with nuclear receptors occurs (NR boxes) are shown in yellow.

with model 8 and model 10 of EID-1 showed the highest score of interaction (model 8, rpscore = 7.13; model 10, rpscore = 7.08).

Inspection of the binding surfaces of SHP and EID-1 models reveals a complementary of charged residues which is the molecular basis of strong electrostatic interactions (Figs. 5 and 6).

The above complementarity is achieved on the model 8 of EID-1 with the presence of an acidic patch constituted by Asp70, Glu71, Asp73, Asp74, Asp77, Asp78, Glu80, Glu83, Glu84 and Glu85. Similarly, a cluster of acidic residues define the interaction surface of model 10. This cluster comprises Glu62, Glu68, Asp70, Asp73, Asp74 and Glu76.

The EID-1 binding surface of SHP is composed by helix H12, the N-terminal loop connecting helix H1 to helix H3 (L1-3) and helix H3. Several positive charged residues contribute to the interaction with EID-1 models. In the complex of SHP with model 8, the interaction surface is constituted by Arg36 (L1-3), Arg38 (L1-3), Arg42 (L1-3), Arg54 (H3), Arg57 (H3) and Arg257 (H12). Similarly, the binding surface of the complex between SHP and model 10 of EID-1 is defined by Arg34 (L1-3), Arg36 (L1-3), Arg38 (L1-3), Arg71 (H3) and Arg257 (H12).

Table 2
Docking score (rpscore) of EID-1 models. Best scoring solution, average value and standard deviation of the top 50 solutions are shown

Fold	Best rpscore	Average	S.D.
Model 1	5.87	4.21	0.64
Model 2	6.80	4.39	0.51
Model 3	6.10	4.17	0.48
Model 4	6.70	4.47	0.74
Model 5	5.74	4.48	0.42
Model 6	5.75	4.30	0.51
Model 7	5.60	3.90	0.55
Model 8	7.13	4.58	0.79
Model 9	6.05	4.76	0.44
Model 10	7.08	4.87	0.57

4. Discussion

The small heterodimer partner (SHP) is an atypical nuclear receptor lacking the ligand-independent activation domain and the DBD. The expression of SHP gene is regulated by a number of nuclear receptors including FXR, SF-1, HNF-4α, LRH-1, ERα and ERRγ. Once expressed in the cell, gene's product inhibits the transcriptional activity of ER, AR, CAR, RXR, GR, LXR and ERRγ. Interestingly, it has been reported that SHP stimulates the transcription function of peroxisome proliferator-activated receptor-γ (PPARγ) through a direct interaction with the DBD of the receptor.

Conversely, the repression mechanism of SHP involves several actions including competition with coactivators binding on the AF-2 of nuclear receptors and recruitment of transcriptional inhibitors.

In the present work, we exploited homology modelling techniques and molecular docking experiments to investigate an in silico model of SHP's repression mechanism.

Beside competition with coactivators binding on the AF-2 surface of nuclear receptors, SHP recruits transcriptional inhibitors to accomplish its repression function. Recently, it has been reported that the corepressor EID-1 selectively interacts with SHP through an interaction domain comprising residues 54–120 [30]. EID-1 is a nuclear protein involved in the block of p300 coactivation function and inhibition of muscle differentiation. Beside SHP, EID-1 does not interact with other nuclear receptors [31,32]. Thus, it may form hetero-trimer complexes where SHP bridges nuclear receptors to achieve its

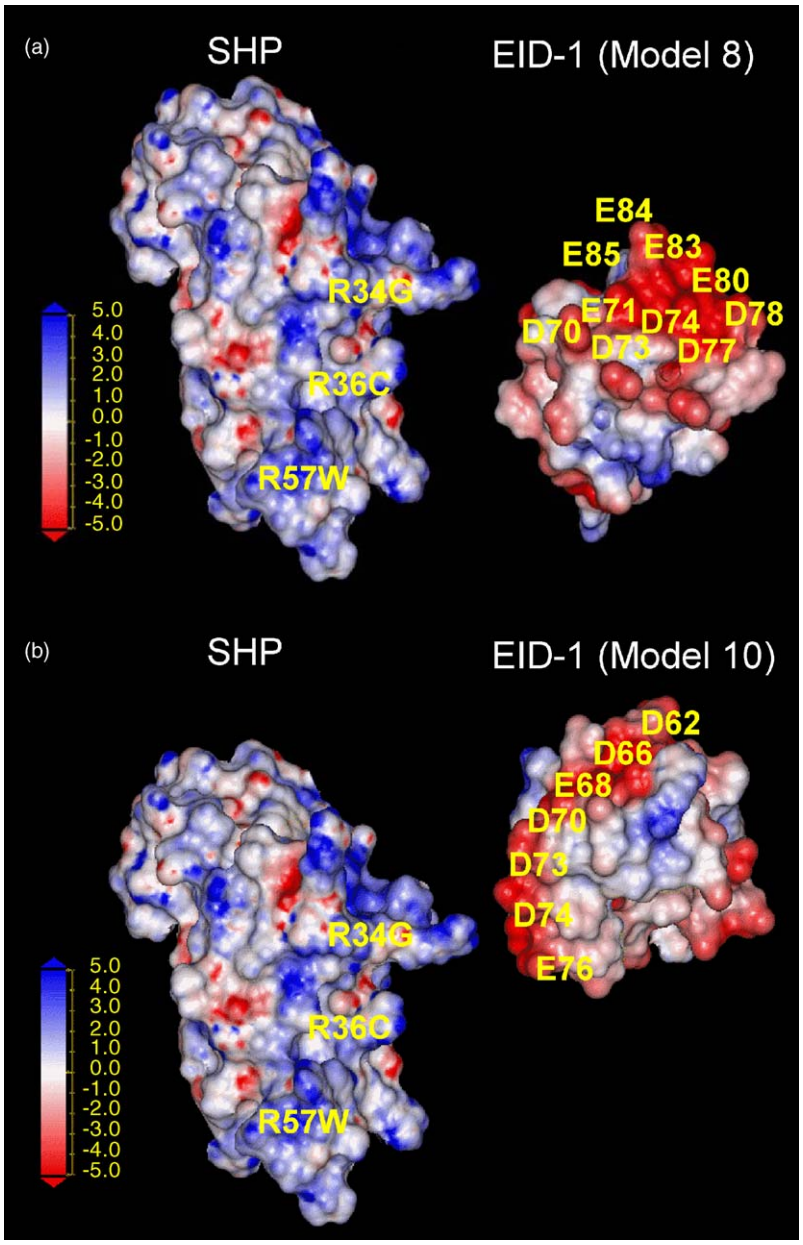

Fig. 6. Electrostatic potential analysis of the binding interfaces between SHP and model 8 (a) and SHP and model 10 (b).

transcriptional inhibition function [49]. To investigate the molecular basis of interaction between SHP and EID-1, we exploited the current *state of the art* of homology modelling techniques to construct 3D models of SHP and interaction domain of EID-1 (residues 54–120).

Our similarity search reveled that the Ultraspiracle receptor (USP) could be a good template to construct a homology model of SHP (see Section 3). A 3D model of SHP, based on the crystal structures of HNF-4α and ERRγ, has been recently published [49]. In this model, helix H12 is in an agonistic conformation and the large loop insertion between helix H6 and H7 (128–139) is modelled in a random coil conformation.

In nuclear receptors, helix H12 contains the activation function AF2 and its conformational state, upon ligand binding, is involved in the recruitment of coactivators/corepressors. Although no SHP ligands have been identified, we thought that the stabilization of an antagonistic conformation of H12 would be the basis of the recruitment of transcriptional inhibitors in SHP. A strong stabilization of an antagonistic conformation of H12 is observed in the crystal structure of USP [46]. Here, helix H12 is locked in a resting conformation through the interaction with the N-terminal loop L1-3. Hence, USP structure would be a suitable template to build an antagonistic conformational model of SHP.

The large non-conserved region (residues 110–138) containing the NR box 2 was modelled using the ab initio prediction Robetta server since several explored alignments failed to assign a correct fold to this region (Fig. 1b). Interestingly, an alpha helix fold was assigned to residues 118–122 (NR box 2).

This is in agreement with the conformation found in crystal structures of coactivators in complex with nuclear receptors. Indeed, it is conceivable to assume an alpha helix conformation as the bioactive conformation to interact with nuclear receptors in competition with coactivators on the AF-2 binding surface. It should be mentioned that also NR box 1 and 3 are endowed with alpha helix conformations according to the relative secondary structure elements of aligned residues in USP. The final 3D model of SHP was refined according to the computational protocol reported in the Section 2.

No homologs were identified for the sequence domain of EID-1. Again, we used Robetta server to assign 10 possible folds to the region 54–120 of EID-1. Molecular docking experiments were carried out for each assigned fold of EID-1 and SHP. Results reveal that top 50 solutions of each docking experiment show a unique spatial distribution. They are clustered around the helix H12 of SHP (only models 8 and 10 are shown for clarity in Fig. 4, see below). Thus, beside whatever is the natural fold of EID-1, the aminoacidic composition of the studied domain determines a preferential interaction with helix H12 of SHP. These data agree the experimental observation about the lost ability of SHP to interact with EID-1 upon deletion of helix H12 [30]. To gain insight into the molecular basis of such interaction, we investigated the solutions with the best docked score among the 10 folds of EID-1. Thus, complexes of SHP with model 8 and model 10 of EID-1 showing the highest score of interaction (model 8, rpscore = 7.13; model 10, rpscore = 7.08) were analyzed. The electrostatic potential analysis of the binding interface of these complexes pinpoints the existence of complementary charged residues which make strong electrostatic interactions (Figs. 5 and 6). In particular, this complementarity is achieved on models of EID-1 with the presence of an acidic patch of residues comprising Glu62, Glu68, Asp70, Glu71, Asp73, Asp74, Glu76, Asp77, Asp78, Glu80, Glu83, Glu84 and Glu85. Basic residues localized on the helix H12, the N-terminal loop connecting helix H1 to helix H3 (L1-3) and helix H3 of SHP are the counterpart of the above acidic patch. In particular, depending on the solution considered, we identified Arg34 (L1-3), Arg36 (L1-3), Arg38 (L1-3), Arg42 (L1-3), Arg54 (H3), Arg57 (H3), Arg71 (H3) and Arg257 (H12) as key residues of such interactions. Noteworthy, mutations of SHP gene associated with a function impairment of its product comprise some of these basic residues; these are Arg34, Arg36 and Arg57 [20,21]. Furthermore, Båvner et al., investigating the binding mode of EID-1 to a set of SHP mutants, reported that the EID-1 binding surface is located on helices H3 and H12 of SHP [30]. Taken together, these data support our work and pinpoint the validity of using an homology model of SHP based on the structure of USP which presents the unique folding of its N-terminal loop around helix H12. Indeed, only this peculiar fold can explain the detrimental effect of natural occurring missense mutations of SHP such as Arg34Gly and Arg36Cys through the impairment of the recruitment of transcriptional inhibitors such as EID-1. Moreover, the work of Båvner et al. reports that the SHP mutant Ala71Pro (Ala68Pro in our sequence numbering) completely lost the ability of recruiting EID-1 [30]. If we assume that an USP-like fold occurs in SHP, this alanine assumes a critical position since it packs helix H3 with the antagonistic conformation of helix H12 that is, in turn, stabilized through interactions with the N-terminal loop L1-3 (Figs. 4 and 5).

Recently, mutagenesis experiments were carried out to gain insight into the role of the large insertion (residues 128–139) of SHP. In particular, deletion mutant (SHP$\Delta^{128-139}$), several polyalanine mutants and DAX-1 swap mutant of SHP were studied to test their ability in keeping or abolishing the interaction with nuclear receptors (mCAR, LHR-1, ERRγ) or EID-1 [49]. Surprisingly, only the deletion mutant (SHP$\Delta^{128-139}$) showed an impaired interaction with EID-1 and, in turn, a strongly reduced inhibitory function. Hence, the authors claimed that the above insertion loop is involved in the maintenance of structural spacing for the interaction with EID-1. In our model, this loop is far away from the binding surface of EID-1 to claim a direct interaction (Fig. 2). It should be reminded that, according to Båvner and coworkers, the above binding surface experimentally encompasses helices H3 and H12. On this basis, the insertion loop (128–139) does not constitute a contiguous binding surface with helices H3 and H12 even in the SHP model based on HNF-4α and ERRγ folds. Furthermore, the presence of EID-1 interaction in different polyalanine mutants of SHP, pinpoints that sequence length and specificity are not required for such interaction. To explain the reported effect of the large insertion of SHP (128–139) on the interaction with EID-1, an intriguing hypothesis rises from the inspection of USP fold. Indeed, the corresponding region in USP constitutes the binding site of a phospholipid, including residues of β-sheet S1-S2, loop L1-3 and helices H3, H5, H6, H7 and H11. If SHP adopts a similar USP-like fold, it is conceivable that such binding site is also present in SHP structure. In particular, it would be composed by a number of conserved hydrophobic residues and few polar residues (Fig. 7).

Interestingly, three charged residues (Asp137, Arg138 and Arg238), being positioned at the entrance of the hydrophobic cavity, may constitute the head of a gorge that would interact with the polar head of putative phospholipids.

In this scenario, the role of 128–139 insertion would be to maintain the SHP fold and stabilize the antagonistic conformation of helix H12 through ligand (phospholipids?) mediated interactions with helix H3. Indeed, the corresponding region in USP is packed on helix H3 through the presence of phospholipids (Fig. 7). Thus, the replacement of the above insertion with a polyalanine chain or DAX-1 swapped sequence would not disrupt the hydrophobic binding site that, in turn, would maintain the above packing. Conversely, deletion of residues 128–139 would break the hydrophobic pocket resulting in an overall destabilization of SHP fold and loss of the antagonistic conformation of helices H3 and H12. If the existence of such ligand-binding pocket is proven then questions arise: does SHP have an endogenous modulator? Is it a phopholipid? If the hydrophobic pocket exists, it may contain structural phospholipids. A recent work pinpoints that such molecules act as ‘‘fillers’’ stabilizing the fold and

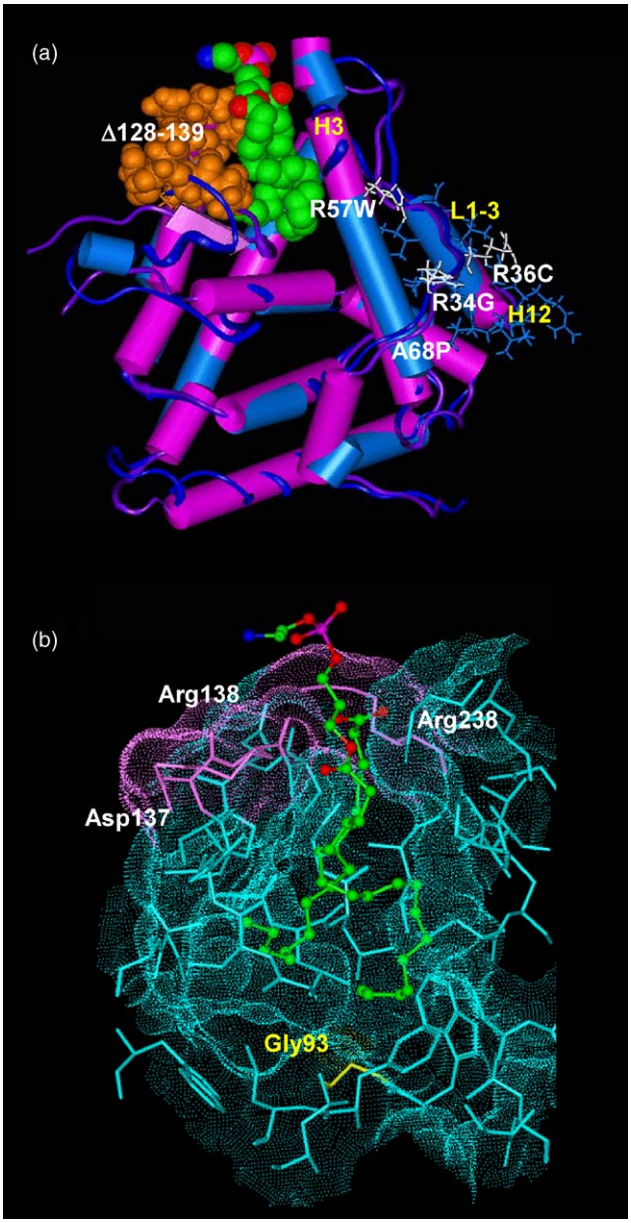

Fig. 7. (a) Superposition of USP (purple) and SHP (blue) structures. Secondary structural motifs and residues of EID-1 binding surface are highlighted. The loop comprising residues 128–139 is shown in orange CPK. The phospholipid complexed with USP structure is shown in atom-type colored CPK. (b) Docking of phosphatidylethanolamine into the phospholipids binding site of SHP structure (see Section 2 for details); charged residues (magenta), Gly93 (yellow).

conformation of the LBD of certain nuclear receptors (USP and retinoic related orphan receptor β) and may not be functional hormones [60]. However, beside the role that a such lipid molecule would cover, proving the existence of a binding site in SHP would represent a breakthrough and allow the design of highly specific synthetic ligands that can be exploited to characterize the functions of SHP.

Very recently, a new variant of SHP with reduced functional activity was reported: the Gly93Asp variant [61].

Glycine 93 is located at the bottom of the putative hydrophobic gorge (Fig. 7). The natural occurring mutation of Gly93 into a charged residue breaks the hydrophobic profile of the gorge hampering the binding of phospholipids and resulting in the loss of the antagonistic conformation of helices H3 and H12 of SHP. These data represent a further clue supporting the existence of a phospholipids binding site in SHP.

5. Conclusions

The investigation of structure and repression mechanism of SHP is a challenging task for a full understanding of nuclear receptor interaction pathways and functions. The lack of an experimental structure of the LBD of SHP prompted us to exploit protein structure prediction techniques and assign putative folds to SHP and its corepressor protein EID-1. In particular, a USP-like fold was assigned to SHP sequence. In this fold helix H12 is frozen in antagonistic conformation through the interaction with the N-terminal loop L1-3.

Both SHP and EID-1 models were used to investigate the transcriptional inhibitor recruitment of SHP. In agreement with available experimental data, results of docking experiments pinpoint that the EID-1 binding surface is located on helices H3, H12 and the N-terminal loop L1-2 of SHP.

The binding interface comprises complementary charged residues. Among these, Arg34, Arg36 and Arg57 were identified as missense mutations in SHP gene leading to impaired function of the product protein. Hence, the USP-like fold of SHP explains the above observation through an impaired recruitment of transcriptional inhibitors. Furthermore, embracing the occurrence of the USP-fold in SHP sequence leads to the existence of unexpected phospholipids (?) binding site in SHP. Noteworthy, this hydrophobic pocket allows a plausible explanation of the effect of loop mutations (residues 128–139) of SHP on EID-1 recruitment. Indeed, the replacement of this large loop with a polyalanine chain or DAX-1 swapped sequence does not disrupt the hydrophobic binding site that, in turn, through the presence of ligands maintains a hydrophobic packing with helices H3 and H12. Deletion of residues 128–139, breaking the hydrophobic pocket, destabilizes SHP fold and the antagonistic conformation of helices H3, H12 that, in turn, hamper EID-1 recruitment. The existence of a phospholipids binding site is further supported by the very recent discovery of a novel functionally not active variant of SHP, Gly93Asp. Indeed, Gly93Asp mutation, being positioned at the bottom of the phospholipids binding site, hampers the interaction of SHP with the hydrophobic chain of phospholipids. Again, this mutation would result in the loss of the hydrophobic packing that stabilizes the antagonistic conformation of helices H3 and H12 which leads to the impairment of SHP function.

The above clues rise question about whether or not an endogenous modulator of SHP does exist. Further experimental data are needed to prove or disprove this hypothesis and to answer the above question. However, the existence of a binding site in SHP structure would allow the design of specific synthetic ligands to be used in the characterization of SHP functions and these would find clinical applications in the control of metabolic dysfunctions.

References

[1] J.M. Maglich, A. Sluder, X. Guan, Y. Shi, D.D. McKee, et al. Comparison of complete nuclear receptor sets from the human, Caenorhabditis elegans and Drosophila genomes, Genome Biol. 2 (2001), RESEARCH0029.

[2] R. Mohan, R.A. Heyman, Orphan nuclear receptor modulators, Curr. Top. Med. Chem. 3 (2003) 1637–1647.

[3] T.M. Willson, J.T. Moore, Genomics versus orphan nuclear receptors-a half-time report, Mol. Endocrinol. 16 (2002) 1135–1144.

[4] D.J. Mangelsdorf, C. Thummel, M. Beato, P. Herrlich, G. Schutz, et al. The nuclear receptor superfamily: the second decade, Cell 83 (1995) 835–839.

[5] A. Aranda, A. Pascual, Nuclear hormone receptors and gene expression, Physiol. Rev. 81 (2001) 1269–1304.

[6] V. Giguere, Orphan nuclear receptors: from gene to function, Endocrinol. Rev. 20 (1999) 689–725.

[7] P. Chambon, A decade of molecular biology of retinoic acid receptors, FASEB J. 10 (1996) 940–954.

[8] C.K. Glass, D.W. Rose, M.G. Rosenfeld, Nuclear receptor coactivators, Curr. Opin. Cell Biol. 9 (1997) 222–232.

[9] L. Xu, C.K. Glass, M.G. Rosenfeld, Coactivator and corepressor complexes in nuclear receptor function, Curr. Opin. Genet. Dev. 9 (1999) 140–147.

[10] J.M. Wurtz, W. Bourguet, J.P. Renaud, V. Vivat, P. Chambon, et al. A canonical structure for the ligand-binding domain of nuclear receptors, Nat. Struct. Biol. 3 (1996) 87–94.

[11] A.M. Brzozowski, A.C. Pike, Z. Dauter, R.E. Hubbard, T. Bonn, et al. Molecular basis of agonism and antagonism in the oestrogen receptor, Nature 389 (1997) 753–758.

[12] W. Seol, H.S. Choi, D.D. Moore, An orphan nuclear hormone receptor that lacks a DNA binding domain and heterodimerizes with other receptors, Science 272 (1996) 1336–1339.

[13] H.K. Lee, Y.K. Lee, S.H. Park, Y.S. Kim, J.W. Lee, et al. Structure and expression of the orphan nuclear receptor SHP gene, J. Biol. Chem. 273 (1998) 14398–14402.

[14] W. Chen, E. Owsley, Y. Yang, D. Stroup, J.Y. Chiang, Nuclear receptor-mediated repression of human cholesterol 7alpha-hydroxylase gene transcription by bile acids, J. Lipid Res. 42 (2001) 1402–1412.

[15] S. Sanyal, J.Y. Kim, H.J. Kim, J. Takeda, Y.K. Lee, et al. Differential regulation of the orphan nuclear receptor small heterodimer partner (SHP) gene promoter by orphan nuclear receptor ERR isoforms, J. Biol. Chem. 277 (2002) 1739–1748.

[16] T.T. Lu, M. Makishima, J.J. Repa, K. Schoonjans, T.A. Kerr, et al. Molecular basis for feedback regulation of bile acid synthesis by nuclear receptors, Mol. Cell 6 (2000) 507–515.

[17] Y.K. Lee, K.L. Parker, H.S. Choi, D.D. Moore, Activation of the promoter of the orphan receptor SHP by orphan receptors that bind DNA as monomers, J. Biol. Chem. 274 (1999) 20869–20873.

[18] S. Gupta, R.T. Stravitz, P. Dent, P.B. Hylemon, Down-regulation of cholesterol 7alpha-hydroxylase (CYP7A1) gene expression by bile acids in primary rat hepatocytes is mediated by the c-Jun N-terminal kinase pathway, J. Biol. Chem. 276 (2001) 15816–15822.

[19] B. Goodwin, S.A. Jones, R.R. Price, M.A. Watson, D.D. McKee, et al. A regulatory cascade of the nuclear receptors FXR, SHP-1, and LRH-1 represses bile acid biosynthesis, Mol. Cell 6 (2000) 517–526.

[20] C.C. Hung, I.S. Farooqi, K. Ong, J. Luan, J.M. Keogh, et al. Contribution of variants in the small heterodimer partner gene to birthweight, adiposity, and insulin levels: mutational analysis and association studies in multiple populations, Diabetes 52 (2003) 1288–1291.

[21] H. Nishigori, H. Tomura, N. Tonooka, M. Kanamori, S. Yamada, et al. Mutations in the small heterodimer partner gene are associated with mild obesity in Japanese subjects, Proc. Natl. Acad. Sci. U.S.A. 98 (2001) 575–580.

[22] Y.K. Lee, D.D. Moore, Dual mechanisms for repression of the monomeric orphan receptor liver receptor homologous protein-1 by the orphan small heterodimer partner, J. Biol. Chem. 277 (2002) 2463–2467.

[23] Y.K. Lee, H. Dell, D.H. Dowhan, M. Hadzopoulou-Cladaras, D.D. Moore, The orphan nuclear receptor SHP inhibits hepatocyte nuclear factor 4 and retinoid X receptor transactivation: two mechanisms for repression, Mol. Cell Biol. 20 (2000) 187–195.

[24] L. Johansson, J.S. Thomsen, A.E. Damdimopoulos, G. Spyrou, J.A. Gustafsson, et al. The orphan nuclear receptor SHP inhibits agonist-dependent transcriptional activity of estrogen receptors ERalpha and ERbeta, J. Biol. Chem. 274 (1999) 345–353.

[25] J. Gobinet, G. Auzou, J.C. Nicolas, C. Sultan, S. Jalaguier, Characterization of the interaction between androgen receptor and a new transcriptional inhibitor, SHP, Biochemistry 40 (2001) 15369–15377.

[26] L.J. Borgius, K.R. Steffensen, J.A. Gustafsson, E. Treuter, Glucocorticoid signaling is perturbed by the atypical orphan receptor and corepressor SHP, J. Biol. Chem. 277 (2002) 49761–49766.

[27] C. Brendel, K. Schoonjans, O.A. Botrugno, E. Treuter, J. Auwerx, The small heterodimer partner interacts with the liver X receptor alpha and represses its transcriptional activity, Mol. Endocrinol. 16 (2002) 2065–2076.

[28] H. Nishizawa, K. Yamagata, I. Shimomura, M. Takahashi, H. Kuriyama, et al. Small heterodimer partner, an orphan nuclear receptor, augments peroxisome proliferator-activated receptor gamma transactivation, J. Biol. Chem. 277 (2002) 1586–1592.

[29] L. Johansson, A. Båvner, J.S. Thomsen, M. Farnegardh, J.A. Gustafsson, et al. The orphan nuclear receptor SHP utilizes conserved LXXLL-related motifs for interactions with ligand-activated estrogen receptors, Mol. Cell Biol. 20 (2000) 1124–1133.

[30] A. Båvner, L. Johansson, G. Toresson, J.A. Gustafsson, E. Treuter, A transcriptional inhibitor targeted by the atypical orphan nuclear receptor SHP, EMBO Rep. 3 (2002) 478–484.

[31] W.R. MacLellan, G. Xiao, M. Abdellatif, M.D. Schneider, A novel Rb- and p300-binding protein inhibits transactivation by MyoD, Mol. Cell Biol. 20 (2000) 8903–8915.

[32] S. Miyake, W.R. Sellers, M. Safran, X. Li, W. Zhao, et al. Cells degrade a novel inhibitor of differentiation with E1A-like properties upon exiting the cell cycle, Mol. Cell Biol. 20 (2000) 8889–8902.

[33] Accelrys Insight-II: San Diego, CA.

[34] PHD Predict Protein Server at http://cubic.bioc.columbia.edu/predictprotein/: San Diego, CA.

[35] A. Fiser, A. Sali, Modeller: generation and refinement of homology-based protein structure models, Methods Enzymol. 374 (2003) 461–491.

[36] D.E. Kim, D. Chivian, D. Baker, Protein structure prediction and analysis using the Robetta server, Nucleic Acids Res. 32 (2004) W526–W531.

[37] B.N. Dominy, C.L. Brooks, Development of a generalized born model parametrization for proteins and nucleic acids, J. Phys Chem. B 103 (1999) 3765–3773.

[38] R. Luthy, J.U. Bowie, D. Eisenberg, Assessment of protein models with three-dimensional profiles, Nature 356 (1992) 83–85.

[39] A.L. Morris, M.W. MacArthur, E.G. Hutchinson, J.M. Thornton, Stereochemical quality of protein structure coordinates, Proteins 12 (1992) 345–364.

[40] G. Moont, H.A. Gabb, M.J. Sternberg, Use of pair potentials across protein interfaces in screening predicted docked complexes, Proteins 35 (1999) 364–373.

[41] I. Klapper, R. Hagstrom, R. Fine, K. Sharp, B. Honig, Focusing of electric fields in the active site of Cu–Zn superoxide dismutase: effects of ionic strength and amino-acid modification, Proteins 1 (1986) 47–59.

[42] G.M. Morris, D.S. Goodsell, R.S. Halliday, R. Huey, W.E. Hart, et al. Automated docking using lamarckian genetic algorithm and empirical binding free energy function, J. Comput. Chem. 19 (1998) 1639–1662.

[43] S.F. Altschul, T.L. Madden, A.A. Schaffer, J. Zhang, Z. Zhang, et al. Gapped BLAST and PSI-BLAST: a new generation of protein database search programs, Nucleic Acids Res. 25 (1997) 3389–3402.

[44] WU-BLAST http://www.ebi.ac.uk/blast2/: San Diego, CA.

[45] S.F. Altschul, E.V. Koonin, Iterated profile searches with PSI-BLAST-a tool for discovery in protein databases, Trends Biochem. Sci. 23 (1998) 444–447.

[46] I.M. Billas, L. Moulinier, N. Rochel, D. Moras, Crystal structure of the ligand-binding domain of the ultraspiracle protein USP, the ortholog of retinoid X receptors in insects, J. Biol. Chem. 276 (2001) 7465–7474.
[47] G.M. Clayton, S.Y. Peak-Chew, R.M. Evans, J.W. Schwabe, The structure of the ultraspiracle ligand-binding domain reveals a nuclear receptor locked in an inactive conformation, Proc. Natl. Acad. Sci. U.S.A. 98 (2001) 1549–1554.
[48] S. Przibilla, W.W. Hitchcock, M. Szecsi, M. Grebe, J. Beatty, et al. Functional studies on the ligand-binding domain of Ultraspiracle from Drosophila melanogaster, Biol. Chem. 385 (2004) 21–30.
[49] Y.Y. Park, H.J. Kim, J.Y. Kim, M.Y. Kim, K.H. Song, et al. Differential role of the loop region between helices H6 and H7 within the orphan nuclear receptors small heterodimer partner and DAX-1, Mol. Endocrinol. 18 (2004) 1082–1095.
[50] W. Seol, M. Chung, D.D. Moore, Novel receptor interaction and repression domains in the orphan receptor SHP, Mol. Cell Biol. 17 (1997) 7126–7131.
[51] E.A. Ortlund, Y. Lee, I.H. Solomon, J.M. Hager, R. Safi, et al. Modulation of human nuclear receptor LRH-1 activity by phospholipids and SHP, Nat. Struct. Mol. Biol. 12 (2005) 357–363.
[52] L.A. Kelley, R.M. MacCallum, M.J. Sternberg, Enhanced genome annotation using structural profiles in the program 3D-PSSM, J. Mol. Biol. 299 (2000) 499–520.
[53] L. Rychlewski, L. Jaroszewski, W. Li, A. Godzik, Comparison of sequence profiles. Strategies for structural predictions using sequence information, Protein Sci. 9 (2000) 232–241.
[54] J. Shi, T.L. Blundell, K. Mizuguchi, FUGUE: sequence-structure homology recognition using environment-specific substitution tables and structure-dependent gap penalties, J. Mol. Biol. 310 (2001) 243–257.
[55] D. Fischer, 3D-SHOTGUN: a novel, cooperative, fold-recognition meta-predictor, Proteins 51 (2003) 434–441.
[56] L.J. McGuffin, D.T. Jones, Improvement of the GenTHREADER method for genomic fold recognition, Bioinformatics 19 (2003) 874–881.
[57] J. Gough, K. Karplus, R. Hughey, C. Chothia, Assignment of homology to genome sequences using a library of hidden Markov models that represent all proteins of known structure, J. Mol. Biol. 313 (2001) 903–919.
[58] K. Ginalski, A. Elofsson, D. Fischer, L. Rychlewski, 3D-Jury: a simple approach to improve protein structure predictions, Bioinformatics 19 (2003) 1015–1018.
[59] D. Chivian, D.E. Kim, L. Malmstrom, P. Bradley, T. Robertson, et al. Automated prediction of CASP-5 structures using the Robetta server, Proteins 53 (Suppl. 6) (2003) 524–533.
[60] N. Potier, I.M. Billas, A. Steinmetz, C. Schaeffer, A. van Dorsselaer, et al. Using nondenaturing mass spectrometry to detect fortuitous ligands in orphan nuclear receptors, Protein Sci. 12 (2003) 725–733.
[61] S.M. Echwald, K.L. Andersen, T.I. Sorensen, L.H. Larsen, T. Andersen, et al. Mutation analysis of NR0B2 among 1545 Danish men identifies a novel c.278G>A (p.G93D) variant with reduced functional activity, Hum. Mutat. 24 (2004) 381–387.